



DOI: 10.18720/MCE.85.7

Quasistaticity of the process of dynamic strain of soils

K.S. Sultanov*, P.V. Loginov, S.I. Ismoilova, Z.R. Salikhova

Institute of Mechanics and Seismic Stability of Structures Academy of Sciences of the Republik of Uzbekistan, Tashkent, Uzbekistan

* E-mail: sultanov.karim@mail.ru

Keywords: soil, dynamic loading, waves, stresses, quasi-statics, mechanical characteristics of soil.

Abstract. Mechanical characteristics of soil under static and dynamic strains are determined experimentally. Their accuracy and reliability depends on quasi-static nature of strain process in soil. The independence of experimental results on the wave processes is ensured. Laboratory devices of dynamic loading (DDL) have been used to determine the laws of dynamic strain and mechanical characteristics of soil. The quasi-static nature of strain process in soil on DDL is achieved solving the wave problem corresponding to experiment. Plane wave propagation in soil is considered; its statement is adequate to experiment on DDL. To describe the dynamic strain of soil, the G.M. Lyakhov elastic-viscoplastic model has been adopted. The system of differential equations in partial derivatives of hyperbolic type, describing the wave process, has been solved by the method of characteristics and finite difference method in an implicit scheme. The changes in wave parameters over time for different sections of soil layer have been obtained by numerical solution. The effect of layer thickness on wave parameters and on quasi-static process is shown by experiments. Quantitative and qualitative influence of mechanical characteristics of soil on wave parameters is determined. Analyzing results, it has been established that the main factors determining the quasi-static process are the parameters of dynamic load and the thickness of soil layer in DDL. The dependence of mechanical characteristics of soil on quasistatic nature of dynamic strain in DDL is shown. Conditions to ensure the quasi-static process of strain in soil sample under dynamic compression on DDL are obtained.

1. Introduction

Stability and seismic resistance of buildings and structures (especially earth and underground structures) are directly related to the strength of soil under static and dynamic loads. Therefore, the study of strength and mechanical properties of soil is a pressing issue throughout the world. Strength characteristics of soil, as is well known, mainly include the coefficient of cohesion and the angle or coefficient of internal friction of soil. In contrast to strength characteristics, mechanical characteristics of soils are related to the laws of soil strain. These include the modulus of elasticity, Poisson's ratio, modulus of unloading, soil viscosity coefficient, etc. These or other mechanical and strength characteristics of soil make it possible to determine and calculate strength and stability of soil as the foundations for the buildings and structures; of earth structures such as dams, dykes, the walls of open pits, slopes and dumps; of underground structures located in different soil conditions. The strength and mechanical characteristics of soil are determined experimentally.

A great amount of publications are devoted to experimental study of strength and mechanical characteristics of soil. Strength characteristics of various soils and rocks under static loads have been experimentally defined in [1–3].

In [1], strength characteristics of loess soils stabilized by silica nanoparticles were determined. It was shown that it increased the strength characteristics of soil. In [2], strength characteristics of soil were

Sultanov, K.S., Loginov, P.V., Ismoilova, S.I., Salikhova, Z.R. Quasistaticity of the process of dynamic strain of soils. Magazine of Civil Engineering. 2019. 85(1). Pp. 71–91. DOI: 10.18720/MCE.85.7.

Султанов К.С., Логинов П.В., Исмоилова С.И., Салихова З.Р. Квазистатичность процесса динамического деформирования грунтов // Инженерно-строительный журнал. 2019. № 1(85). С. 71–91. DOI: 10.18720/MCE.85.7



This open access article is licensed under CC BY 4.0 (<https://creativecommons.org/licenses/by/4.0/>)

determined depending on water saturation by the direct shear test and the triaxial compression method. In [3], strength characteristics of soil were defined in relation to the stability of slopes.

Experimental determination of strength characteristics of soil under dynamic loads in field conditions was given in [4, 5]. In [4], the shear resistance of soft clay was determined at the free fall of a steel sphere of 0.25 m diameter into water. The measuring unit, located inside the sphere, measured the response to sphere motion at fall and penetration into soil. The obtained acceleration measurement data allowed determining strength characteristics of soil. In [5], by a method similar to the one in [4], strength characteristics of the seabed were determined at various velocities of the impact of a steel ball.

Experimental determination of mechanical characteristics of soil under static loads was given in [6–9]. In [6], the elastic modulus of a granular material was determined at low values of strain, depending on the diameter of the grain particles. It had been established that the Young modulus was practically independent of the diameter of particles of granular material. In [7], the strain modulus was determined by compressive and pressing tests of soil samples. Under triaxial cyclic loading, the strain characteristics of soil were defined in [8]. Mechanical viscoelastic characteristics of geosynthetic materials under static stresses were determined in [9].

Mechanical characteristics of soils and rocks under dynamic loads have been defined in [10–23] in laboratory and field conditions.

In [10], mechanical characteristics of brittle soils were determined under loading rates of axial stress equal to 0.05–10 kN/s in laboratory conditions. It was established that the modulus of elasticity of soil increased with an increase in loading rate. In [11], elastic properties of clay soil were determined by measuring the velocities of ultrasonic waves of various frequencies propagating in soil. The dynamic modulus obtained experimentally was compared to the static modulus. In [12], mechanical characteristics of soft clay were determined under dynamic loads by the centrifugal modeling method. In [13–15], dynamic parameters of friction and resistance at sliding of dry and water-saturated surfaces of soil and sand were experimentally determined. Mechanical characteristics of a prismatic marble block, pyroclastic rocks and clayey soil were studied by ultrasonic scanning in [16–18].

Mechanical characteristics of soil, based on specific elastic-viscoplastic models, under static and dynamic loads have been determined in [19–23] in laboratory and field conditions.

Complex laws of strain in soils and rocks were given in [24–28], the consideration of applied problems of fracture – in [29], a comparative analysis of mechanical characteristics determined by different methods – in [30] and nonlinear models of soil strain – in [31–35]. The emergence of non-one-dimensional problems of seismic stability of earth structures required experimental data on mechanical characteristics of soils and rocks, especially under dynamic loads.

The values of mechanical characteristics of soil when calculating seismic stability of underground structures were of particular relevance [23]. Without the knowledge of mechanical characteristics of soil under dynamic strain it is impossible to estimate the quantitative parameters of various waves in soil media and rocks [19–23, 33]. The reliability of the values of mechanical characteristics of soils when solving the problems of seismic resistance of aboveground and earth structures (soil dams, levees, walls of open pit, foundations) is very important [36–38].

In field experiments it is almost impossible to obtain repetitions of exactly the same tests in quantities and quality that allow static processing of results. The latter circumstance is very important to prove the reliability of experimental results.

In [21], the authors have created a special device for dynamic loading (DDL) to determine dynamic characteristics of soils. In this case, a soil sample of undisturbed or disturbed structure was tested for shock loads created by a falling weight. The DDL operated on the principle of a compression device for testing soils under static loads. Design description of the DDL and the principles of its operation were given in detail in [21]. The method of experimental determination of mechanical characteristics of soil proposed in [21] allowed serial experiments, the results of which were then processed using the methods of mathematical statistics. As a result, significantly reliable experimental data were obtained for determining mechanical characteristics of soil under dynamic loads [21].

However, in this case, when conducting experiments on dynamic compression of soil samples on the DDL, another problem arose. It laid in the fact that the stress measurement results were affected by the wave process that occurred in a soil sample when it was subjected to a shock load. To accurately measure the stresses in soil under dynamic uniaxial compression on the DDL, it was necessary to ensure the quasistatic nature of the process of soil strain. The quasistatic process of dynamic strain was realized under the conditions

$\frac{d\sigma}{dx} = 0$ and $\frac{d\varepsilon}{dx} = 0$, where σ was the longitudinal stress along the compression x axis, ε was the longitudinal strain along the x axis.

In [21], the conditions for the quasistatic nature of the process of dynamic strain of soil were determined at some theoretical assumptions. According to these conditions, the ratio of the mass of soil sample and the mass of the DDL piston should satisfy the condition of a quasistatic nature given in [21]. The condition of the values of rise time of dynamic load from zero to the maximum should also be satisfied. In [21], the wave process occurring in soil under shock load was not investigated.

Based on the analysis of published sources [1-38], and, particularly, on the results obtained in [19–23, 34], the wave problem which corresponds to the statement of the experiment on the DDL is solved in this paper. In published sources, there is no solution to this problem. The object of the study is the wave process in soil under its dynamic compression and the dynamic stress-strain state of soil.

Theoretical substantiation of the validity of experimental results obtained in laboratory conditions on the device of the DDL type is an actual problem, since the accuracy of calculations on strength and seismic stability of soils and soil structures directly depends on the reliability of mechanical characteristics determined from the results of dynamic compression of soils.

The aim of this study is to theoretically investigate the wave process in a soil sample placed in the DDL soil receiving chamber and to determine the conditions for the quasistatic nature of the process of dynamic strain of a soil sample based on the analysis of wave parameters.

To achieve this goal, the following tasks are solved:

1. Choice and substantiation of the law of soil strain on the DDL. Determination of the basic equations of motion describing the process of dynamic compression of soil and the boundary conditions corresponding to the statement of the experiment on the DDL.
2. Choice of a numerical method for solving the obtained wave equations, its substantiation. Development of the principles for the construction of an algorithm and a program for solving a system of differential equations describing wave processes in soil.
3. Choice and substantiation of the initial values of mechanical characteristics of soil, of the parameters of dynamic load to carry out numerical calculations. Obtaining numerical results characterizing the changes in the parameters of waves in different sections of soil.
4. Analysis of the obtained numerical results of the changes in the parameters of waves in soil, depending on physical and mechanical characteristics of soil and its thickness.
5. Determination of the conditions for the quasistatic nature of dynamic strain in soil on the basis of studies, which ensure the reliability of the results of dynamic experiments on the DDL.

2. Methods

2.1. Statement of theoretical problem corresponding to the experiment on the DDL

The DDL-100 and DDL-150 devices described in [21] have a cylindrical soil receiving chambers with diameters of 0.1 or 0.15 m and a height of 0.03 m, into which a cylindrical soil sample of undisturbed or disturbed structure is placed. The bottom plane of the chamber, where the soil sample rests, is fixed. On the upper plane of the soil sample, there is a piston through which dynamic load created by the impact of load of a certain weight, freely falling along the guide bars, is transferred [21].

The wave pattern of experimental setup on the DDL is quite complicated. On the x axis of a cylindrical soil sample, a load acting from the upper piston varies from zero to maximum and then again to zero. According to the results obtained in [21], one of the conditions to ensure the quasi-static nature of the strain process is the ratio of the rise time of the load to the maximum and the fall time to zero. The rise time of the load should always be less than the fall time. This is a rigor condition to ensure the quasi-static nature of the process of soil strain on the DDL.

The load change is represented here as a half-sinusoid. In this case, the rise time equals to the fall time. This load uniformly acts on the upper plane of the soil layer located in the DDL soil-receiving chamber, which ensures the one-dimensional character of dynamic and static process of soil compression. The side walls of the soil-receiving chamber have sufficient smoothness, which allows the friction forces between soil and side wall to be zero. So, the forces of soil friction on the side surface are neglected.

A layer of soil 0.03 m thick is located at a distance $0-x_*$ along the x axis. At a distance $x = x_*$ there is an upper plane of the lower, absolutely rigid, fixed piston. This plane can be considered as a fixed obstacle.

According to the results of the above experiments, soil is considered to be an elastically viscous-plastic medium.

At $t = 0$, load $\sigma = \sigma(t)$, varying by a sinusoidal law, begins to act on the soil layer. A wave is propagating in undisturbed soil. The front of this wave reaching the lower plane reflects from it. Under the effect of load $\sigma = \sigma(t)$ plastic strains are formed in soil. Consequently, a plastic wave propagates in soil [21].

After load $\sigma = \sigma(t)$ reaches its maximum, one more front is formed – the front of the maximum stress in soil, followed by unloading. At $\sigma = \sigma(t) = 0$ the front of the wave of unloading propagates in soil. The above fronts, reflected from the lower piston ($x = x_*$) and from the upper piston ($x = 0$) form a complex wave pattern.

Due to the fact that load $\sigma = \sigma(t)$ acting on the soil layer is continuous, these fronts are the lines of weak discontinuity, that is, the wave parameters do not have jumps (discontinuities) on these fronts. Only the first derivatives of the wave parameters on these fronts can have discontinuities; therefore, they are called weak discontinuity lines. This circumstance, as will be shown later, greatly simplifies the solution of the theoretical problem corresponding to the dynamic compression of the soil layer on the DDL.

The linearity of wave fronts mainly depends on the specific type of equation of state of soil and on the load. In case of linearity or even piecewise linearity of the equation of state of soil, which determines mechanical characteristics of soil, the wave fronts remain linear under continuous loading. In case of nonlinearity of the equation of state, these fronts are nonlinear. In case of nonlinearity of fronts, the problem of dynamic compression of a soil sample on the DDL is significantly complicated. The wave pattern and, therefore, the statement of the problem corresponding to the case under consideration, directly depends on the equation of state or the law of soil strain, on the basis of which mechanical characteristics of soil are determined.

In [21, 22, 33] it was shown that even at load values of 0.3–0.5 MPa, the process of dynamic strain in experiments demonstrated the elastic-viscoplastic properties of soil. Based on this, a soil model adequate to this process is chosen.

According to the analysis of the equation of state of soil [19–22, 33], the most complete law of soil strain, which takes into account the plastic strain of soil and its viscous properties under volume changes, is the law proposed in [22]. Let us consider this law in the process of strain in loess soil on the DDL, that is define mechanical characteristics of loess soil based on the model given in [22].

The model of an elastic-viscoplastic medium has the following form [22]:

$$\left. \begin{aligned} \frac{d\varepsilon}{dt} + \mu\varepsilon &= \frac{d\sigma}{E_D dt} + \mu \frac{\sigma}{E_S} \quad \text{at } \frac{d\sigma}{dt} > 0, \frac{d\varepsilon}{dt} > 0 \\ \frac{d\varepsilon}{dt} + \mu\varepsilon &= \frac{d\sigma}{E_R dt} + \mu\sigma \left(\frac{1}{E_S} + \frac{1}{E_D} + \frac{1}{E_R} \right) + \mu\sigma_m \left(\frac{1}{E_D} + \frac{1}{E_R} \right) \quad \text{at } \frac{d\sigma}{dt} < 0, \frac{d\varepsilon}{dt} > 0 \\ \frac{d\varepsilon}{dt} &= \frac{d\sigma}{E_R dt} \quad \text{at } \frac{d\sigma}{dt} < 0, \frac{d\varepsilon}{dt} < 0 \end{aligned} \right\} \quad (1)$$

where E_D is the modulus of dynamic compression of soil at $d\varepsilon/dt \rightarrow \infty$,

E_S is the modulus of static compression of soil at $d\varepsilon/dt \rightarrow 0$,

E_R is the unloading modulus, μ is the viscosity parameter, which is related to the viscosity coefficient by the ratio

$$\mu = \frac{E_D E_S}{\eta(E_D - E_S)} \quad (2)$$

where η is the coefficient of soil viscosity under volume changes,

σ_m is the maximum stress in soil particles. Equation (2) was obtained analytically in [22]. The principles and experimental grounds of the model construction (1) and relationship (2) were described in detail in [22].

The parameter η characterizes the dependence of the soil stresses on the strain rate $\frac{d\varepsilon}{dt}$. The value of η was determined experimentally [22, 34].

Strain ε , as applied to the experiments on the DDL-150, explicitly determines the volume change in the soil layer. Therefore, it can be considered as a volume strain, and σ as the pressure. In this case $\sigma = -P$, where P is the pressure. From this it follows that the equation of state of soil (1) is the law of variation of the spherical part of the stress tensor, that is, the law of the volume strain of soil. From (1) it is clear that in this case the basic mechanical characteristics of soil are E_D, E_S, E_R and μ .

Until now, the values of mechanical characteristics of soils mentioned above or other ones (based on other equations of soil state) have been determined directly from the results of experiments on the readings of the diagrams of soil compression.

However, dynamic compression of soil on the DDL is a rather complicated process; it is accompanied by a rather complex wave pattern. The values of stress and strain at different points of the soil sample along the x axis are affected by both the waves reflected from the lower and upper pistons and by their superposition. As a result, we can get the wrong values of mechanical characteristics of soil, just their apparent values, formed as a result of the superposition of incident and reflected waves.

Ensuring the quasi-static nature of the process of dynamic strain in soil eliminates the influence of wave processes on the values of mechanical characteristics of soil on the DDL. Despite the assessment of the quasi-static nature of the process of soil strain on the DDL [21], this condition needs to be assessed by studying the wave processes in a soil sample under dynamic load on the DDL.

To determine the quasistatic process of soil strain on the DDL, it is necessary to solve the equation of motion, which has the form:

$$\rho_0 \frac{\partial v}{\partial t} - \frac{\partial \sigma}{\partial x} = 0, \quad \frac{\partial v}{\partial x} - \frac{\partial \varepsilon}{\partial t} = 0, \quad (3)$$

where ρ_0 is the initial density of soil,

v is the velocity of soil particles under compression.

The equation of one-dimensional soil motion in the DDL (3) is successively closed by the equations of state of soil (1). In the closed system of equations (3), (1), the unknowns are σ , ε and v , called the parameters of waves in soil or the parameters of stress-strain state of soil in the DDL.

To solve the system of differential equations (3), (1), it is necessary to state the initial and boundary conditions. The initial conditions of the problem are zero, since before the loading, the soil on the DDL is at rest, that is, it is considered undisturbed.

The boundary conditions of the problem, corresponding to the statement of the experiment, are the following: at $x = 0$ the upper plane of the soil layer in the DDL is affected by load $\sigma = \sigma(t)$ due to the motion of the upper piston; at $x = x_*$ the lower piston is fixed, that is $v = 0$, the velocity of the soil particles at this boundary is zero.

Mathematical formulation of the boundary conditions is as follows.

$$\left. \begin{aligned} \sigma &= \sigma(t) \text{ at } x = 0, 0 < t < t_* \\ \sigma &= 0 \text{ at } x = 0, t > t_* \\ v &= 0 \text{ at } x = x_* \end{aligned} \right\} \quad (4)$$

where t_* is the duration of load.

On the front of the incident wave the following condition is met:

$$\langle \sigma \rangle = 0, \quad \langle \varepsilon \rangle = 0, \quad \langle v \rangle = 0 \quad (5)$$

at $x = ct$

where c is the velocity of longitudinal wave propagation in soil,

$\langle \sigma \rangle, \langle \varepsilon \rangle, \langle v \rangle$ are the jumps in the wave parameters.

In case of the equations of state (1), the front line $x = ct$ and the lines of all other fronts are straight lines. This follows from the linearity of the equations that make up the law of soil strain (1).

Thus, the process of dynamic strain of a soil sample located in the DDL is described by the system of equations (1), (3). Having solved the system of equations (3), (1) with boundary conditions (4), (5) and zero initial conditions, the dynamic stress-strain state of soil can be determined.

2.2. Method and algorithm for solving the problem of dynamic compression of soil on the DDL

The system of equations (3), (1) is a hyperbolic one [22, 23]. At present, it is not possible to obtain an analytical solution for these equations. Therefore, we will use the numerical method of finite differences. First, following [22, 23], we will use the method of characteristics. The system of equations (3), (1) is a hyperbolic one and it has real characteristics and characteristic relations.

As a result of applying the method of characteristics, partial differential equations (3), (1) are reduced to ordinary differential equations. The application of the finite difference method to ordinary differential equations improves the accuracy of their solution compared to differential equations in partial derivatives [22, 23].

The successive closure of equations (3) by the equations of the law of soil strain (1) leads to three systems of equations that have the following characteristic relations on the characteristic lines:

$$\left. \begin{aligned} d\sigma - c\rho_0 dv &= c^2 \rho_0 \mu \left(\varepsilon - \frac{\sigma}{E_S} \right) dt, \quad \frac{dx}{dt} = +c \\ d\sigma + c\rho_0 dv &= c^2 \rho_0 \mu \left(\varepsilon - \frac{\sigma}{E_S} \right) dt, \quad \frac{dx}{dt} = -c \\ d\sigma - c\rho_0 dv &= c^2 \rho_0 \mu \left(\varepsilon - \frac{\sigma}{E_S} \right) dt, \quad \frac{dx}{dt} = 0 \end{aligned} \right\} \quad (6)$$

$$\left. \begin{aligned} d\sigma - c_1 \rho_0 dv &= c_1^2 \rho_0 \mu \left(\varepsilon - \sigma \left(\frac{1}{E_S} + \frac{1}{E_R} - \frac{1}{E_D} \right) - \sigma_m \left(\frac{1}{E_D} - \frac{1}{E_R} \right) \right) dt, \quad \frac{dx}{dt} = +c_1 \\ d\sigma + c_1 \rho_0 dv &= c_1^2 \rho_0 \mu \left(\varepsilon - \sigma \left(\frac{1}{E_S} + \frac{1}{E_R} - \frac{1}{E_D} \right) - \sigma_m \left(\frac{1}{E_D} - \frac{1}{E_R} \right) \right) dt, \quad \frac{dx}{dt} = -c_1 \\ d\sigma + c_1^2 \rho_0 d\varepsilon &= c_1^2 \rho_0 \mu \left(\varepsilon - \sigma \left(\frac{1}{E_S} + \frac{1}{E_R} - \frac{1}{E_D} \right) - \sigma_m \left(\frac{1}{E_D} - \frac{1}{E_R} \right) \right) dt, \quad \frac{dx}{dt} = 0 \end{aligned} \right\} \quad (7)$$

$$\left. \begin{aligned} d\sigma - c_1 \rho_0 dv &= 0, \quad \frac{dx}{dt} = +c_1 \\ d\sigma + c_1 \rho_0 dv &= 0, \quad \frac{dx}{dt} = -c_1 \\ d\sigma - c_1^2 \rho_0 d\varepsilon &= 0, \quad \frac{dx}{dt} = 0 \end{aligned} \right\} \quad (8)$$

where $c = \sqrt{E_D / \rho_0}$; $c_1 = \sqrt{E_R / \rho_0}$.

Using the method of characteristics, the system of differential equations (3), (1) is replaced by the system (6)–(8).

The derivation of the equations of characteristics and characteristic relations is given in detail in [22]. The system of equations (6)–(8) has been solved on a computer, with the transition to dimensionless variables and parameters using an implicit finite-difference scheme. The transition to dimensionless variables reduces the errors in numerical calculations associated with their accumulation in calculations when using large numbers.

The transition to dimensionless variables is carried out according to the formula:

$$\left. \begin{aligned} t^0 &= \mu t, \quad x^0 = \mu x / c, \quad \sigma_0 = \sigma / \sigma_{\max} \\ v^0 &= v / v_{\max}, \quad \varepsilon^0 = \varepsilon / \varepsilon_{\max} \\ v_{\max} &= \sigma_{\max} / c \rho_0, \quad \varepsilon_{\max} = \sigma_{\max} / E_D \end{aligned} \right\} \quad (9)$$

where σ_{\max} is the maximum value of the load acting at $x = 0$, that is, in the upper plane of the soil layer.

In dimensionless variables, the basic equations take the form

$$\frac{\partial v^0}{\partial t^0} - \frac{\partial \sigma^0}{\partial x^0} = 0, \quad \frac{\partial v^0}{\partial x^0} - \frac{\partial \varepsilon^0}{\partial t^0} = 0 \quad (10)$$

The laws of soil strain (1) in new variables is written as

$$\left. \begin{aligned} \varepsilon^0 + \frac{d\varepsilon^0}{dt^0} &= \frac{d\sigma^0}{dt^0} + \gamma\sigma^0 \\ \varepsilon^0 + \frac{d\varepsilon^0}{dt^0} &= \beta \frac{d\sigma^0}{dt^0} + \sigma^0(\gamma + \beta - 1) + \sigma_m^0(1 - \beta) \\ \frac{d\varepsilon^0}{dt^0} &= \beta \frac{d\sigma^0}{dt^0} \end{aligned} \right\} \quad (11)$$

where $\gamma = E_D / E_S$, $\beta = E_D / E_R$.

The characteristic relations in the dimensionless form are determined by the following equations:

$$\left. \begin{aligned} &\text{at } d\sigma^0 / dt^0 > 0, \quad d\sigma^0 / dt^0 < d\varepsilon^0 / dt^0 \\ d\sigma^0 \pm dv^0 &= (\varepsilon^0 - \gamma\sigma^0) dt^0 \text{ along the lines } dx^0 / dt^0 = \pm 1 \\ d\sigma^0 - d\varepsilon^0 &= (\varepsilon^0 - \gamma\sigma^0) dt^0 \text{ along the lines } dx^0 / dt^0 = 0 \end{aligned} \right\} \quad (12)$$

$$\left. \begin{aligned} &d\sigma^0 / dt^0 < 0, \quad d\sigma^0 / dt^0 < \beta d\varepsilon^0 / dt^0 \\ d\sigma^0 \pm \frac{dv^0}{\sqrt{\beta}} &= \frac{1}{\beta} [\varepsilon^0 - (\gamma + \beta - 1)\sigma^0 - (1 - \beta)\sigma_m^0] dt^0, \quad dx^0 / dt^0 = \pm \frac{1}{\sqrt{\beta}} \\ d\sigma^0 - \frac{d\varepsilon^0}{\beta} &= \frac{1}{\beta} [\varepsilon^0 - (\gamma + \beta - 1)\sigma^0 - (1 - \beta)\sigma_m^0] dt^0, \quad dx / dt = 0 \end{aligned} \right\} \quad (13)$$

$$\left. \begin{aligned} &\text{at } d\sigma^0 / dt^0 < 0, \quad d\sigma^0 / dt^0 = \beta d\varepsilon^0 / dt^0 \\ \sqrt{\beta} d\sigma^0 \pm dv^0 &= 0, \quad dx^0 / dt^0 = \pm \frac{1}{\sqrt{\beta}} \\ \sqrt{\beta} d\sigma^0 - d\varepsilon^0 &= 0, \quad dx^0 / dt^0 = 0 \end{aligned} \right\} \quad (14)$$

From equations (12)–(14) it is seen that the solution domains in plane x^0, t^0 have three sets of characteristic lines. Depending on the solution domain and conditions in (12)–(14), the incline of the characteristic lines varies, but they always remain straight lines.

The boundary conditions at dimensionless variables are:

$$\left. \begin{aligned} \sigma^0 &= \sigma(t) / \sigma_{\max} \text{ at } x^0 = 0, \quad 0 \leq t^0 \leq \mu t_* \\ \sigma(t) &= \sigma_{\max} \sin(\pi t / t_*) \\ \sigma^0 &= 0 \text{ at } x^0 = 0, \quad t^0 > \mu t \\ \sigma^0 = 0, \quad \varepsilon^0 = 0, \quad v^0 = 0 &\text{ at } x^0 = t^0 \\ v^0 &= 0 \text{ at } x^0 = x_0^* \end{aligned} \right\} \quad (15)$$

In case of the equation of state of soil (1) and boundary conditions (15), all front lines are the lines of weak discontinuity. There are no “jumps” in wave parameters on these fronts.

The absence of strong discontinuities at the wave fronts makes it possible to perform calculations on the time layers (Figure 1) by the “through” counting method, which does not take these fronts into account in the algorithm. This is the advantage of this statement of the problem.

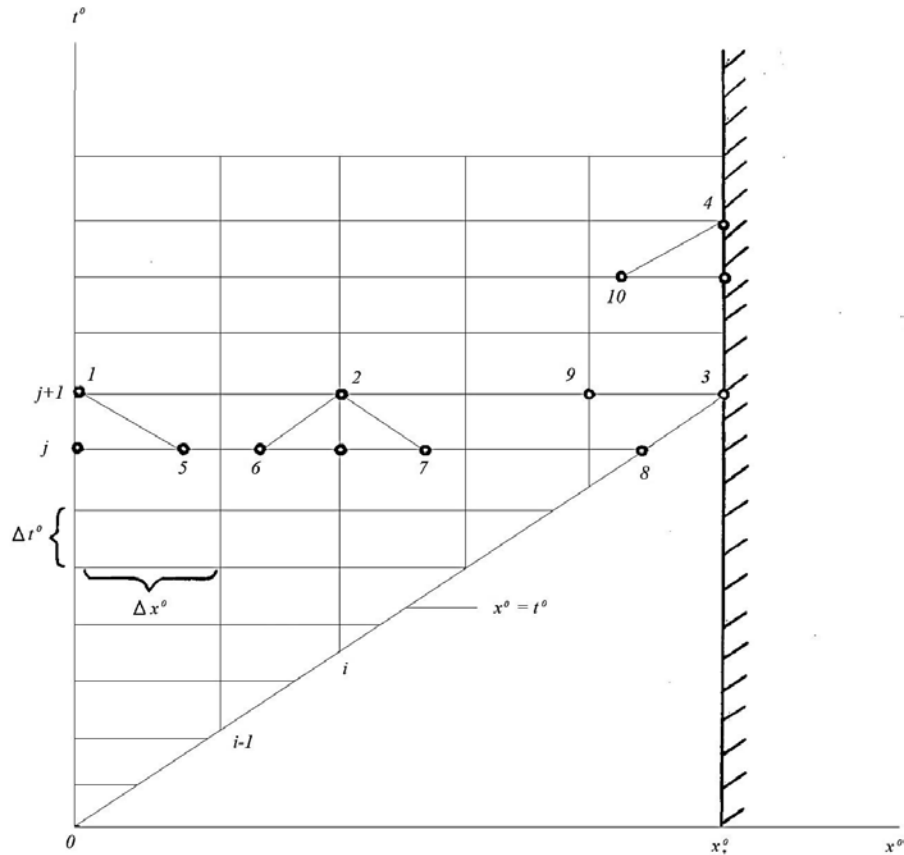


Figure 1. Discretization scheme for the solution domain and the types of calculation points.

In the calculation domain, in plane x^0, t^0 there are four types of calculation points 1–4: point 1 in cross section $x^0 = 0$, internal point 2, point 3 at the wave front, point 4 at the lower piston of the DDL. The wave parameters at these points are to be determined. Equation (12)–(14) are written in a difference form. For example, for point 2 in case of equation (12) they have the form:

$$\left. \begin{aligned} (\sigma_2^0 - \sigma_6^0) + (v_2^0 - v_6^0) &= 0.5[\varepsilon_2^0 + \varepsilon_6^0 - \gamma(\sigma_2^0 + \sigma_6^0)]\Delta t^0 \\ (\sigma_2^0 - \sigma_7^0) - (v_2^0 - v_7^0) &= 0.5[\varepsilon_2^0 + \varepsilon_7^0 - \gamma(\sigma_2^0 + \sigma_7^0)]\Delta t^0 \\ (\sigma_2^0 - \sigma_i^0) + (\varepsilon_2^0 - \varepsilon_i^0) &= 0.5[\varepsilon_2^0 + \varepsilon_i^0 - \gamma(\sigma_2^0 + \sigma_i^0)]\Delta t^0 \end{aligned} \right\} \quad (16)$$

Similarly, using the boundary conditions (15), the difference equations could be written for points 1, 3, 4 and for other cases. The values of the parameters in time layer j are considered known. Parameters at points 5, 6, 7, 8, 10 (Figure 1) are determined by linear interpolation. In time layer $j + 1$, the parameter values are to be determined.

In the layer $j + 1$, the parameters of the near-front point 9 are also determined by interpolation.

In computer-aided calculations, the values of Δt^0 and Δx^0 are given according to the Courant condition. For this problem it has the form:

$$\frac{\Delta x^0}{\Delta t^0} \geq 1/\sqrt{\beta} \quad (17)$$

Condition (17) is necessary and sufficient so that the characteristics do not go beyond the boundaries of the quadrilateral cell. Otherwise, the stability of computer calculation is lost.

Thus, the solution of a system of equations (12) – (14) with boundary conditions (15) is reduced to solving a system of linear algebraic equations of (16) type. In (16), $\sigma_2^0, \varepsilon_2^0, v_2^0$ are the unknowns.

First, equation (16) is solved relative to these unknowns. Further, using these solutions and similar solutions for other types of points, an algorithm for solving the problem is built.

On the basis of the above algorithm and the solution of the problem shown in calculation scheme in Figure 1, a program for solving the problem has been compiled in the Pascal algorithmic language in the DELPHI environment. The developed program is implemented on a computer. The stability of the algorithm of problem solution is verified by a numerical experiment using different values of Δt^0 and Δx^0 and initial parameters of the problem. The results of numerical experiments have shown that the stability of computational scheme and algorithm is fully ensured by the Courant condition. The reliability and accuracy of the methods used for solving equations (1) – (2), i.e. the method of characteristics with the successive application of the finite difference method according to an implicit scheme is considered in [22, 34]. The drawn up program in each cell of the discrete grid (Figure 1) is controlled by the condition (17). The results of comparison of numerical solutions of the problem of plane wave propagation in elastic-viscoplastic medium (1) with an analytical solution in elastic and elastic-plastic media are given in [34]. These results [34] show that the method used makes it possible to obtain numerical solutions of wave problems with high accuracy and reliability.

2.3. Validation of the algorithm and program for problem solution

The algorithm and program for problem solution developed above are verified by comparing the results of numerical solutions and experiments. To do this, the full-scale experiment given in [34] is chosen. In [34], the propagation of an explosive wave in loess soil has been studied experimentally in full-scale (field) conditions. The statement of the experiment in [34] is one-dimensional. The behavior of loess soil is described by equations (1)–(3). The initial conditions in the experiment are zero, the boundary conditions (4), in this case, have the following form [34]:

$$\begin{aligned} \sigma &= \sigma_{\max} (1 - t / \theta)^3 & 0 \leq t \leq \theta \\ \sigma &= 0 & t \geq \theta \end{aligned} \quad (18)$$

where $\sigma_{\max} = 30 \cdot 10^5$ Pa is the maximum value, and $\theta = 10^{-2}$ is the time of action of explosive load. Mechanical characteristics of soil, as an elastic-viscoplastic medium (1), have been determined on the basis of field experiments in [34]. They are as follows: $\gamma = 4$, $\beta = E_D / E_R = 0.4$; $\mu = 1000 \text{ s}^{-1}$, $\mu\theta = 10$.

Load (18) in a dimensionless form, on the basis of equations (9) has the form

$$\begin{aligned} \sigma^0 &= (1 - t^0 / \mu\theta)^3 & 0 \leq t^0 \leq \mu\theta \\ \sigma^0 &= 0 & t^0 \geq \mu\theta \end{aligned} \quad (19)$$

Numerical solution of the problem of explosive wave propagation in soil initiated by load (19) is obtained using the algorithm and program developed above. Dimensionless numerical solutions are converted to dimensional ones, taking into account the experimental values of parameters $\varepsilon_{\max} = 0.116$; $c = 100 \text{ m/s}$; $\rho_0 = 1500 \text{ kg/m}^3$, $\sigma_{\max} = 30 \cdot 10^5 \text{ Pa}$, $E_D = 280 \cdot 10^5 \text{ Pa}$, $E_s = 70 \cdot 10^5 \text{ Pa}$, $E_R = 700 \cdot 10^5 \text{ Pa}$, given in [34].

In calculation program for solving experimental problem, the distance from the initial section of soil to the obstacle x_* is taken as sufficiently large ($x_* = 100 \text{ m}$), then, the statements of the experiment and theoretical problem completely coincide. The statement of the experiment and the results obtained are given in detail in [34].

Figures 2 and 3 show the graphs of dependences $\sigma(t)$ and $\varepsilon(t)$. Curves 1 and 2 correspond to experiments [34] related to distances $x = 0.2 \text{ m}$ and 0.6 m from the initial section of soil $x = 0$, where the load acts (19). Curves 1* and 2* refer to the results of numerical calculations obtained according to the developed algorithm and program.

Figure 4 shows the results of comparisons of soil compression diagram $\sigma(\varepsilon)$, constructed using experimental and theoretical (numerical calculations) dependences $\sigma(t)$ and $\varepsilon(t)$, shown in Figures 2 and 3. Here curve 1 is an experiment, curve 2 is a numerical solution obtained based on the program for solving the problem under consideration.

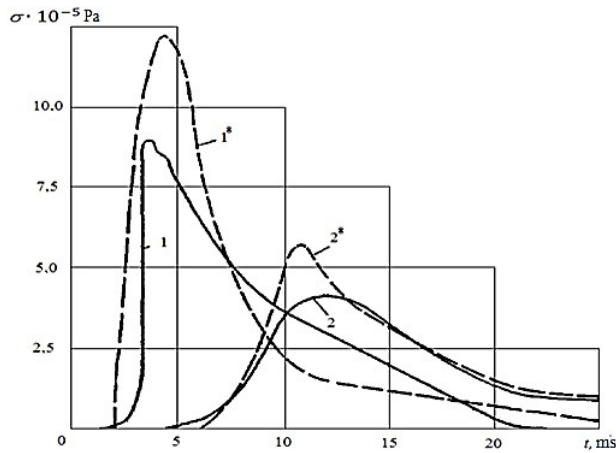


Figure 2. Change in stresses over time. Solid lines – experiment, dotted lines – theory.

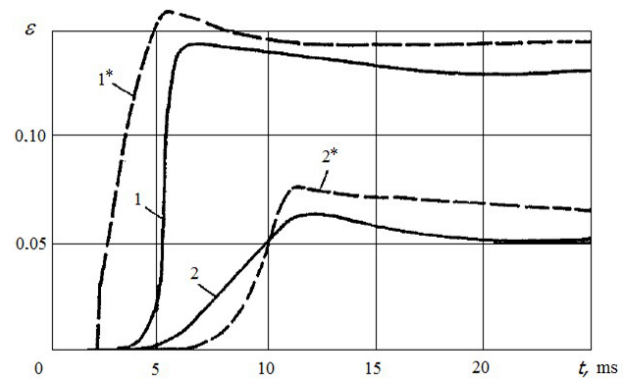


Figure 3. Change in strain over time. Solid lines – experiment, dotted lines – theory.

From Figures 2–4 it can be seen that the experiment and the numerical solution obtained on the basis of the algorithm and computer program developed above coincide qualitatively and satisfactory. The maximum stress values differ by 30 %, and the maximum strain values by 15–20 %, which is quite satisfactory and is within the limits of experimental accuracy. The scatter of data is 15–30 %. This result is quite acceptable for testing the theory and a full-scale experiment in the dynamics of soil [18–23].

Thus, the results of comparison of theoretical calculations with the data of a full-scale experiment show that the developed algorithm and program for calculating the problem in question give quite satisfactory results. This means that the algorithm and program developed above for solving the problem in question allow the study of wave processes in soil within the limits of the problem statement, described by equations (1)–(3).

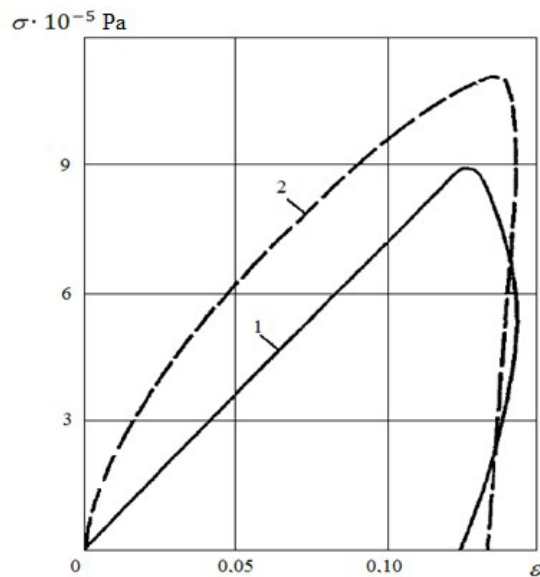


Figure 4. Diagram $\sigma(\epsilon)$, curve 1 – experiment, curve 2 – numerical solution.

3. Results and Discussion

3.1. Results of calculations of wave parameters and patterns of strain of loess soil samples, placed in the DDL

The patterns of plane wave propagation in soil as in an elastic-viscoplastic medium were theoretically investigated in [22, 23, 36]. Theoretical problem according to the above method, in case when soil is a linear viscoelastic medium (a standard-linear body), has been numerically solved using the method of characteristics [22, 34]. In [22, 34], the problems of wave interaction with a moving non-deformable obstacle in a viscoplastic medium – soil – were considered. The wave interaction with a deformable obstacle in a viscoelastic medium was studied in [23].

The interaction of a continuous compression wave with a rigidly fixed obstacle in an elastic-visco-plastic medium has not yet been studied. So, the solution to the problem considered here is obtained for the first time.

The considered problem of the interaction of a continuous plane compression wave with a rigidly fixed obstacle in an elastic-viscous-plastic medium – soil – is studied on the DDL to determine the conditions of

quasistatic process of dynamic strain of soil. The compiled algorithm and the program for solving the problem make it possible to investigate (on the results of numerical solutions) the change in wave parameters in soil and the patterns of soil strain, not only in relation to the DDL tests.

The main parameters (initial data) of the problem to conduct the calculations are:

– soil characteristics – $\gamma = E_D / E_S$, $\beta = E_D / E_R$, ρ_0 , c , μ ;

– load characteristics – σ_{\max} , t_* ;

– distances from the initial section of soil to the obstacle – x_* .

Table 1. Options for computer calculations at various values of the parameters.

№ of option	γ	β	x_*, m	t_*, s	μ, s^{-1}
1	2	0.5	2.8	0.1	100
2	4	0.5	2.8	0.1	100
3	2	0.5	0.28	0.1	100
4	2	0.5	0.03	0.1	100
5	4	0.5	0.03	0.1	100
6	1.05	0.5	0.03	0.1	1000
7	2	0.25	0.03	0.01	100
8	2	0.5	0.03	0.01	100
9	2	0.5	0.03	0.001	100

Options for computer calculations at various values of the parameters are given in Table 1. They are selected based on the parameters of seismic load in loess soils [23]. Based on the results of experiments [23], the value of maximum load σ_{\max} for all the options is taken as equal to 0.5 MPa. The initial density of soil ρ_0 is 1500 kg/m³, the velocity of longitudinal wave propagation is $c = 100$ m/s. Values of ρ_0 and c for option 6 have been changed: $\rho_0 = 2000$ kg³/m, $c = 1000$ m/s. Option 6 corresponds to elastic-plastic soil, where the density of soil and, accordingly, the velocity of longitudinal wave propagation in soil are more significant than in elastic-viscoplastic soil [23].

When choosing the options listed in Table 1, possible values of $\gamma, \beta, x_*, t_*, \mu$ have been taken into account [21–23].

The value of the modulus of dynamic compression E is determined by formula $E_D = c^2 \rho_0$, the static compression modulus by $E_S = E_D / \gamma$, and the unloading modulus by $E_R = E_D / \beta$.

Numerical solution of the problem is obtained in a dimensionless form. Then, using relations (9), they are transformed into dimensional ones.

Let us consider the results of computer calculations.

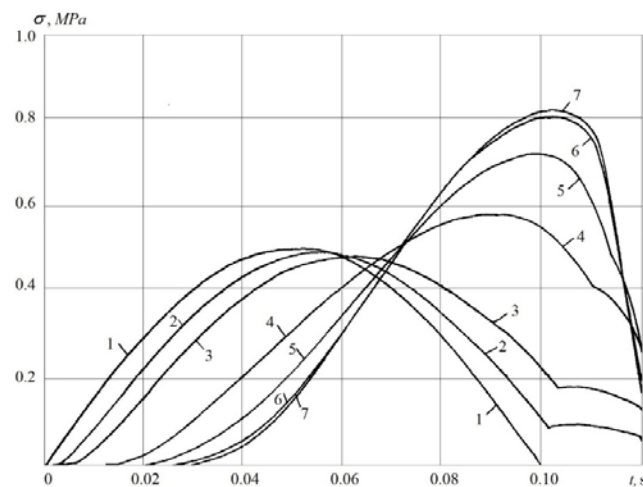


Figure 5. Stress variations in soil sections: 1) $x = 0$; 2) $x = 0.28$; 3) $x = 0.56$; 4) $x = 1.15$; 5) $x = 1.2$; 6) $x = 2.55$; 7) $x = 2.8$ m.

Figure 5 shows the longitudinal stress σ variation over time t for different sections of soil for option 2 (Table 1). Curves 1-7 refer to the sections of soil at $x = 0; 0.28; 0.56; 1.15; 1.2; 2.55$ and 2.8 m, respectively. At $x = x_* = 2.8$ m there is a fixed and non-deformable obstacle.

In theoretical calculations there is a possibility of arbitrary positioning of the lower piston of device. In option 2, the obstacle (lower piston) is specifically set aside at a distance of $x_* = 2.8$ m to consider the pattern of change in wave parameters in soil.

Note that in dependencies $\sigma(t)$, hereinafter, the stress σ should be understood as the compression stress. In the figures, a negative sign in front of σ is omitted for simplicity. Similarly, the strain under compression is taken as positive.

As seen from Figure 5, under conditions (15), at $x = 0$ a half-period of sinusoidal load is acting on soil (curve 1). At a distance of $x = 2.83$ m there is an obstacle. In this option, at $t_* = 0.1$ s of load action, the wave 3.5 times runs to the obstacle and back. As a result of the superposition of waves reflected from the lower and upper boundaries, different values of stresses are observed on different sections of the soil layer. On the obstacle, the maximum stress is 1.6 times greater than in the initial section (curve 7). In other sections of soil, the maximum stress value is also greater than in the initial section. A similar picture is observed at dependencies $\varepsilon(t)$ (Figure 6). Here, the maximum strain is reached on the obstacle (curve 7). The values of residual strains in soil sections are significant. Curves 1–7 refer to the same distances as shown in Figure 5.

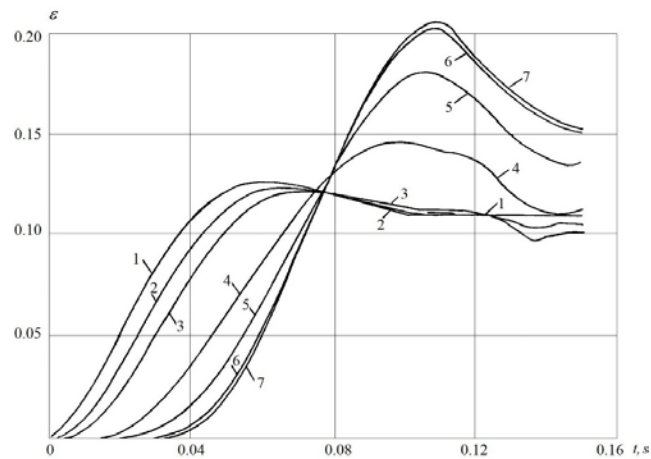


Figure 6. Strain variation in soil sections: 1) $x = 0$; 2) $x = 0.28$; 3) $x = 0.56$; 4) $x = 1.15$; 5) $x = 1.2$; 6) $x = 2.55$; 7) $x = 2.8$ m.

Dependencies $\sigma(t)$ and $\varepsilon(t)$ given in Figures 5 and 6 show that the changes in stress and strain in different sections of soil under dynamic loads differ. This circumstance should be taken into account when determining mechanical characteristics of soil from similar experiments.

The change in velocity (mass velocity) over time at the same sections of soil for option 2 is shown in Figure 7. Here, the maximum velocity is reached in the cross section $x = 0$. Later, it decreases, and on the obstacle the values of velocities are zero (line 7).

The change in soil displacements at different sections of soil is shown in Figure 8. The initial section of soil under loading, as expected, shows significant displacements (curve 1). Subsequent sections of soil are less displaced (curves 2-6), and on the obstacle the displacement of soil is naturally absent (line 7).

As seen from Figures 5–8 the wave processes in soil, in this option, are of significant importance. When conducting similar experiments (at considerable thickness of the soil layer) to define mechanical characteristics of soil under dynamic load, it is necessary to take into account the effect of wave processes on the values of stress and strain in soil.

Compression diagrams for soil sections (option 2) are shown in Figure 9. Here elastic-viscoplastic strain of soil is observed in all sections of soil. However, quantitatively these dependences $\sigma(\varepsilon)$ for different sections of soil differ. At the values of initial data of option 2, significant residual strains of soil have been observed. The maximum stress values are slightly behind the maximum strain values. As seen from Figure 9, the soil compression diagrams on sections $x=0$ and $x=2.8$ m differ significantly. Mechanical characteristics of soil, determined on the basis of these diagrams, will also differ significantly.

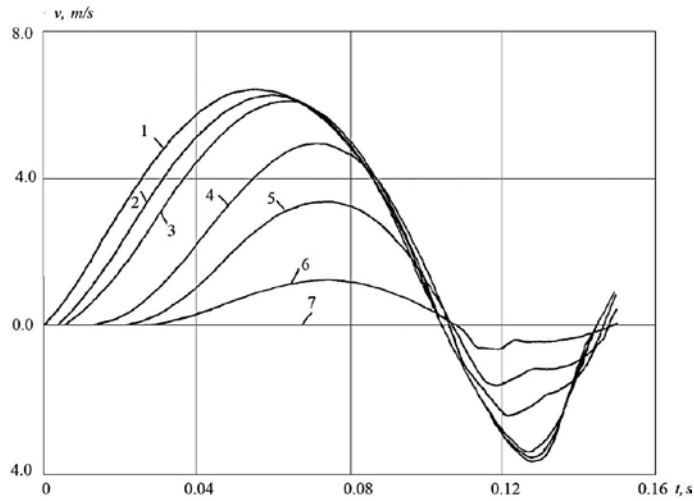


Figure 7. Changes in particle velocity in soil sections: 1) $x = 0$; 2) $x = 0.28$; 3) $x = 0.56$; 4) $x = 1.15$; 5) $x = 1.2$; 6) $x = 2.55$; 7) $x = 2.8$ m.

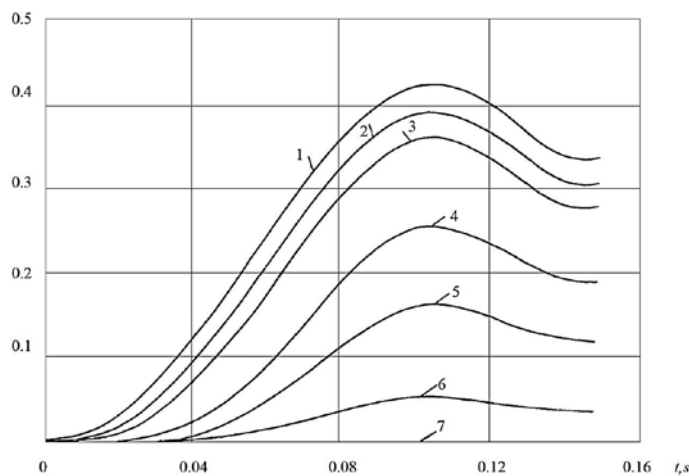


Figure 8. Displacements of soil particles in sections: 1) $x = 0$; 2) $x = 0.28$; 3) $x = 0.56$; 4) $x = 1.15$; 5) $x = 1.2$; 6) $x = 2.55$; 7) $x = 2.8$ m.

In this case, the values of mechanical characteristics of soil are influenced by the wave process in soil. These mechanical characteristics of soil are not true. To obtain true values of mechanical characteristics of soil, it is necessary to exclude the effect of wave processes on the stress-strain state of soil under dynamic loading. That is, the soil compression diagrams in all sections of soil should be identical.

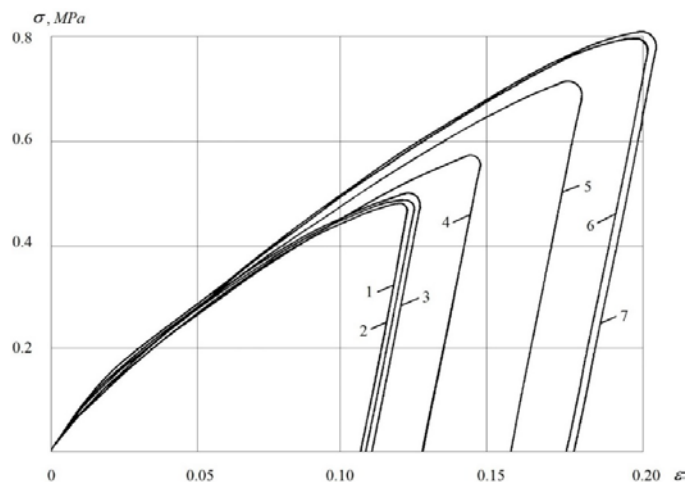


Figure 9. Stress-strain dependences for soil sections: 1) $x = 0$; 2) $x = 0.28$; 3) $x = 0.56$; 4) $x = 1.15$; 5) $x = 1.2$; 6) $x = 2.55$; 7) $x = 2.8$ m.

Results of calculations for option 2 at $\gamma = 4$ (Figures 5–9) show that an increase in γ corresponding to an increase in viscous properties of soil leads to a decrease in the maximum stress values as compared to option 1. The values of maximal and residual strains increase with increase in γ . The increase in γ also leads to an increase in the velocity values of soil particles. Accordingly, the values of soil displacement increase.

At increase in γ , the compression diagrams $\sigma(\varepsilon)$ for considered soil sections do not qualitatively change, but they differ quantitatively as compared to option 1. In option 2, the values of maximum stresses are less, the values of residual strains are greater, and the lag of maximum strains from maximum stresses is greater as compared to option 1. In quantitative terms, the double increase in γ of considered sections of soil leads to 1.1 times decrease in maximum stresses, to approximately 2 times increase in maximum strains and residual strains, to approximately 1.5 times increase in velocity and displacement.

In case of 10 times reduction of the distance from initial section to the obstacle (option 3) at $\gamma = 2$, $\beta = 0.5$, a significantly different wave pattern is observed in the soil layer as compared to options 1 and 2 (Figure 10).

Figure 10 shows the stress changes for the sections of soil layer at $x_* = 0; 0.028; 0.056; 0.15; 0.2; 0.254$ and 0.28 m for curves 1-7, respectively. Here $x_* = 0.28$ m, that is, the obstacle is at a distance of 0.28 m from the initial section of soil. As seen from Figure 10, in this case the stress values in all sections of the soil layer are almost the same (curves 1-7). At decrease in x_* , the strain values for all cross sections merge into one curve (Figure 11).

The change in velocity of soil particles for the considered cross sections with decreasing distance to the obstacle becomes more complex (Figure 12). Here the results of multiple wave reflections from the rigid surfaces of the upper and lower pistons are observed. During the time of load effect the wave 35 times runs back and forth from the initial section to the obstacle. The value of displacements in this case is important; it is about 10 times less than in options 1 and 2. Under the same dynamic load, a decrease in thickness of the soil layer leads to a decrease in soil displacement, while the strains remain almost the same in all sections of soil (Figure 11). As expected from Figures 10 and 11, for option 3 the dependences $\sigma(\varepsilon)$ for all cross sections of the layer become identical.

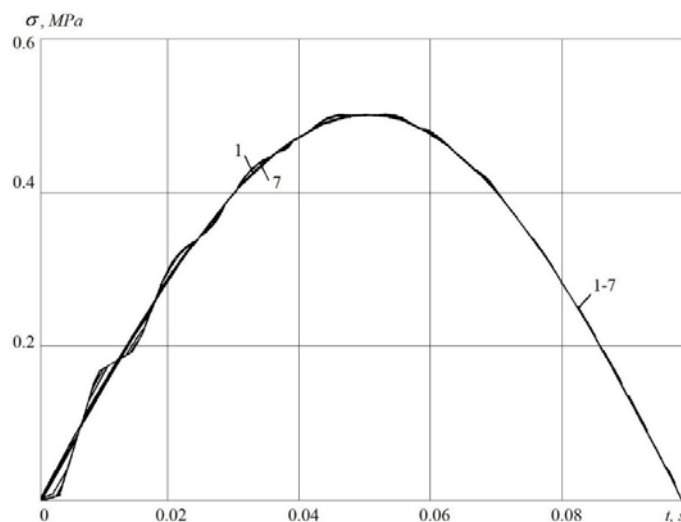


Figure 10. Stress variation in soil sections at $x_* = 0.28$ m.

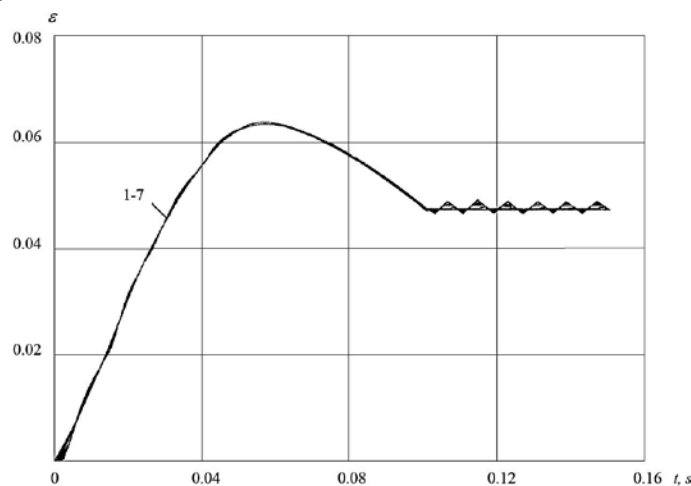


Figure 11. Strain variation in soil sections at $x_* = 0.28$ m

The results of calculations of option 3 (Figures 10–12) show that even at the soil layer thickness $x_* = 0.28$ m the conditions for quasi-static nature of soil compression for a given dynamic load are met, that is, the stress and strain values for all soil sections become identical. However, this circumstance depends not only on the thickness of the soil layer, but also on the parameters of dynamic load.

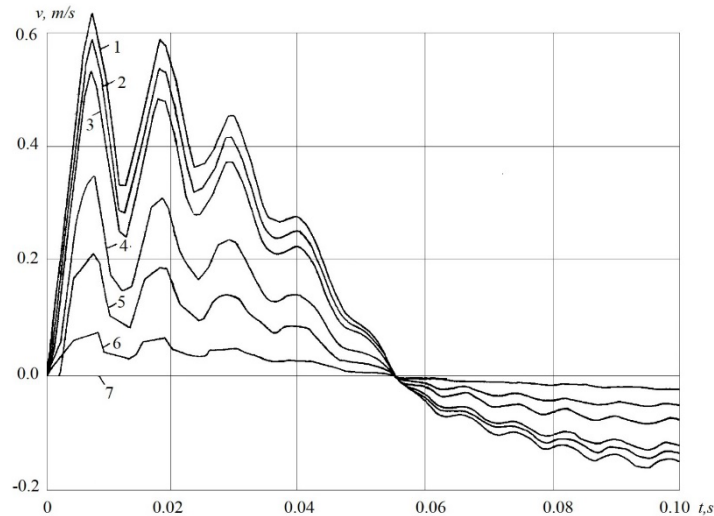


Figure 12. Velocity variation in soil sections: 1) $x = 0$; 2) $x = 0.028$; 3) $x = 0.056$; 4) $x = 0.15$; 5) $x = 0.2$; 6) $x = 0.255$; 7) $x = 0.28$ m.

In general, the patterns of changes in wave parameters in soil, as shown by the results of the above numerical solutions, depend on the characteristics of soil, on the thickness of the soil layer and, of course, on the characteristics of dynamic load. The latter is especially important to ensure the quasi-static nature of the process of soil strain in experiments. The study of this issue is considered on the examples for options 4–9 (Table 1).

3.2. Quasistatic nature of the process of soil strain on the DDL

As shown above, the quasistatic process of dynamic strain in soil on the DDL depends on the thickness of the soil layer. At considerable thicknesses of the layer $x_* > 0.3$ m and the time of load action $t_* \leq 0.1$ sec, we can assume that the quasistatic nature of the process of soil strain is not ensured (options 1 and 2). This means that the values of stress and strain in different sections of soil differ significantly. To refer these differences in experiments to the scattering of experimental data will be incorrect and will lead to incorrect results in statistical processing.

So, it is very important to exclude the differences in dependences $\sigma(t)$ and $\varepsilon(t)$ related to the effect of waves reflected from the lower piston. In experiments, complete agreement of dependences $\sigma(t)$ and $\varepsilon(t)$, fixed by sensors installed above and below the soil layer, is necessary. This is ensured, first of all, by the condition of a quasi-static process of dynamic strain in soil. In other words, when dynamic load is applied, the soil layer strains almost statically, that is, in all its points stress and strain values are identical. Such dynamic strain in soil is called a quasi-static strain.

The thickness of the soil layer in the experiments on the DDL equals to $x_* = 0.03$ m [21]. Based on this, when choosing options 4–9 (Table 1), x_* is taken as equal to 0.03 m. Using as example the calculation of option 4, consider the change in wave parameters in soil layer of 0.03 m thick and load time of $t_* = 0.1$ s.

In options 4–9, the changes in wave parameters are given in the sections of soil layers: $x = 0$; 0.0028; 0.0056; 0.015; 0.02; 0.0255 and 0.03 m.

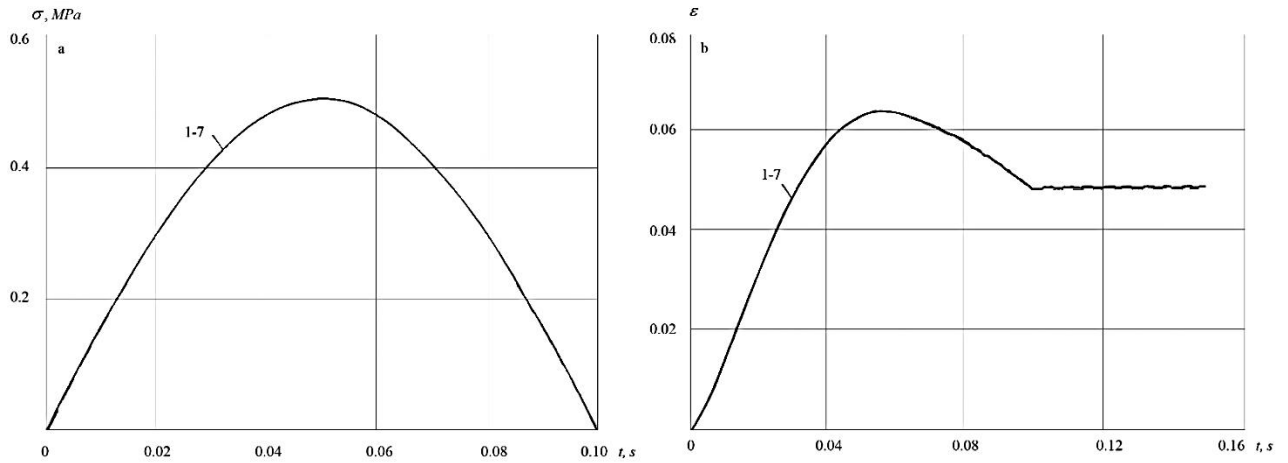


Figure 13. Variation in stress (a) and strain (b) in soil sections at $x_* = 0.03$ m.

Figure 13a shows the dependencies $\sigma(t)$ related to the above distances (curves 1–7) for option 4 (Table 1). As seen from Figure 13a, at time of load action $t_* = 0.1$ s, the dependencies $\sigma(t)$ for all sections of soil are exactly the same. This proves the complete quasistatic nature of the process of soil strain on the DDL at a given dynamic load. In option 4, the dependencies $\varepsilon(t)$ for the considered sections of the soil layer also completely agree (Figure 13b).

The changes in particle velocity are completely different for the considered soil sections. At time of load action of 0.1 s (option 4), the wave 333 times runs back and forth in the soil layer. As a result of multiple reflections of waves from the upper and lower pistons and their superposition, we have a complex pattern of velocities. The displacements of soil particles in the considered soil sections are also different. In this case, the maximum displacement of the upper piston is approximately 0.002 m.

Increasing the value of γ at constant values of other parameters (option 5) does not affect the dependencies $\sigma(t)$. Dependencies $\varepsilon(t)$ change quantitatively. Maximum and residual values of strains increase. Dependencies $v(t)$ become less sensitive to the reflected waves. The maximum values of the velocity of soil particles increase by an order of magnitude.

At increase in γ , the compression diagram $\sigma(\varepsilon)$ remains the same for all sections of soil. The increase in γ (which corresponds to an increase in viscous and plastic properties of the medium) does not affect the quasi-static nature of the process of soil strain on the DDL, as the results of calculations show.

A decrease in γ , which corresponds to an increase in elastic properties of soil, does not affect the quasi-static nature of the process of soil strain on the DDL as well. This case is considered on the example of option 6. Here $\gamma = 1.05$, accordingly: $c = 1000$ m/s and $\mu = 1000$ s⁻¹. The other parameters remain unchanged. At the loading time of $t_* = 0.1$ s, the wave more than 3000 times runs through a layer of soil of 0.03 m thick. Dependencies $\sigma(t)$ and $\varepsilon(t)$ for all sections of soil are completely identical.

It is characteristic that with an increase in elastic properties of soil, the value of residual strain at the lower piston is about two times less than in other sections. This is due to the increase in number of wave reflections from the lower piston. In this case, the displacements of soil particles become significantly smaller than in cases when $\gamma = 2$ and $\gamma = 4$.

At $\gamma = 1.05$, the soil compression diagram $\sigma(\varepsilon)$ corresponds to the diagram of elastic-plastic medium. Here the values of residual strains decrease, the maximum values of stresses and strains coincide over time. However, the quasistatic nature of the process of soil strain is not violated.

The effect of an increase in parameter $\sigma(\varepsilon)$ on the calculation results is shown on the example of option 7. Here, $\beta = 0.25$. The remaining values of the parameters are the same as in option 4. A decrease in β , which corresponds to an increase in plastic properties of soil, leads to an increase in residual strain of soil. A decrease of β does not affect the values of the maximum displacements.

According to the soil compression diagram, a decrease in β does not affect the quasi-static process of soil strain on the DDL.

Reducing the load time t_* by 10 times (option 8) leads to a noticeable violation of the quasi-static nature of the process of soil strain. In this case, the stress values in the sections of soil layer differ by 10–15 %. Similar differences are observed in the values of strains. In dependencies $v(t)$ and $u(t)$ high-frequency oscillations associated with a much shorter load time are observed. Violation of the quasi-static nature of the process is also observed in dependencies $\sigma(\varepsilon)$. The quasi-static nature of the process is noticeably disturbed in the stage of unloading of the soil layer.

Reducing the load time t_* by 100 times (option 9), as compared to option 4, leads to an explicit violation of quasi-static process of soil strain on the DDL. At $t_* = 0.001$ s, the values of stresses and strains in the considered sections of the soil layer differ significantly. On the upper and lower pistons, their values differ about twice. At a decrease in time of action of dynamic load, the values of stress and strain are significantly affected by the waves reflected from the lower piston. At $t_* = 0.001$ s, the pattern of changes in dependencies $v(t)$ and $u(t)$ has also changed. There are no high-frequency oscillations.

At $t_* = 0.001$ s, dependencies $\sigma(\varepsilon)$ change significantly. The process of soil strain becomes an elastic-plastic one. The quasistatic nature of the process is completely violated under soil unloading.

The results of calculations of the options listed in Table 1 allow us to estimate the quasistatic nature of the process of soil strain on the DDL. To do this, let us determine half the wavelength, propagating in soil on the DDL:

$$\lambda = ct_*. \quad (20)$$

Introduce the ratio of half the wavelength λ to the thickness of the soil layer. The data obtained for options 1–9 are shown in Table 2.

Table 2. The data obtained for options 1–9.

№ of option	c , m/s	t_* , s	x_* , m	λ , m	λ / x_*
1	100	0.1	2.8	10	3.5
2	100	0.1	2.8	10	3.5
3	100	0.1	0.28	10	35
4	100	0.1	0.03	10	333
5	100	0.1	0.03	10	333
6	1000	0.1	0.03	100	3333
7	1000	0.1	0.03	10	333
8	100	0.01	0.03	1	33
9	100	0.001	0.03	0.1	3.3

According to the results of calculations (options 1–9), for options 1, 2, 9, the quasistatic process of soil strain on the DDL is not observed. For options 3 and 8, the quasistatic process is observed satisfactorily. For options 4–7, the quasi-static process is observed with high accuracy.

Based on the data of Table 2, to maintain the quasi-static nature, the following condition must be met:

$$\lambda / x_* = \lambda / \delta_o > 50 \quad (21)$$

When the ratio of half the wavelength to the thickness of the soil layer δ is more than 50, the quasi-static nature of the process of soil strain under dynamic compression on the DDL is fully ensured. The greater the ratio λ / δ , the more accurate the quasi-static nature of the process of soil strain. Consequently, the reliability of the results of experiments obtained on the DDL increases.

4. Conclusions

1. A problem on propagation and interaction of plane waves with a rigidly fixed obstacle is set; the problem corresponds to dynamic compression of soil samples on a device of dynamic loading (DDL), designed to define the laws of dynamic strain and on their basis to determine mechanical characteristics of soil.

2. An algorithm and a program for solving the wave problem on a computer using the characteristic method, the finite difference method in an implicit scheme have been developed. The stability conditions of the algorithm and the program for solving the problem are determined and realized on a computer.

3. For known physical-mechanical characteristics of loess soils and parameters of the DDL-150, numerical results have been obtained in the form of changes in stress, strain, particle velocity and displacements over time for different sections of soil.

4. The changes in the stress-strain state have been analyzed for different values of dynamic load, of the soil layer thickness in the DDL and physical-mechanical characteristics of soil.

5. The conditions for the quasistatic nature of dynamic strain in soil on the DDL have been determined depending on the parameters of load, the wavelength and the thickness of the soil layer in the DDL. It is established that when the ratio of half the wavelength to the thickness of the soil layer in the DDL is 50 or more, the quasi-static nature of the process of dynamic strain in soil on the DDL is fully ensured.

References

1. Qingfend, L., Chengrui, C., Benhai, Z., Bo, M.. Loess Soil Stabilization by Means of SiO₂ Nanoparticles. *Soil Mechanics and Foundation Engineering*. 2017. Vol. 54. No. 6. Pp. 409–413.
2. Nguyen, F.Z. Issledovaniya zavisimosti prochnostnykh svoystv grunta ot yego fizicheskogo sostoyaniya [Study of Dependence of Soil Strength Properties on its Physical State]. *Magazine of Civil Engineering*. 2012. No. 9 (35). Pp. 23–28. (rus)
3. Goldin, A.L., Nguyen, F.Z. Postroyeniye trayektorii napryazheniy dlya nenasyshchennogo grunta pri konsolidirovannom nedrenirovannykh ispytaniyakh v stabilometre [Construction of a Stress Trajectory for Unsaturated Soil in Consolidated-Un-drained Tests in a Stabilometer]. *Magazine of Civil Engineering*. 2012. No. 9 (35). Pp. 35–40. (rus)
4. Morton, J.P., O'Loughlin, C.D., White, D.J. Estimation of soil strength in fine-grained soils by instrumented free-fall sphere tests. *Géotechnique*. 2016. Vol. 66. No. 12. Pp. 959–968.
5. Chow, S.H., Airey, D.W. Soil strength characterisation using free-falling penetrometers. *Géotechnique*. 2013. Vol. 63. No. 13. Pp. 1131–1143.
6. Tadao, E. Effects of grading and particle characteristics on small strain properties of granular materials. *Soils and Foundations*. 2016. Vol. 56. No. 4. Pp. 745–750.
7. Ignatova, O.I. Deformation characteristics of the Jurassic clayey soils of Moscow. *Soil Mechanics and Foundation Engineering*. 2009. Vol. 46. No. 5. Pp. 196–201.
8. Aleksandrov, A.S. Plasticheskoye deformirovaniye granodioritovogo shchebnya i peschano-graviynoy smesi pri vozdeystvii trekhosnoy tsiklicheskoy nagruzki [Plastic Strain of Granodiorite Crushed Stone and Sand-Gravel Mix under the Influence of a Three-Axis Cyclic Load]. *Magazine of Civil Engineering*. 2013. No. 4(39). Pp. 22–34. (rus)
9. Loginova, I.I., Artomonova, D.A., Stolyarov, O.N., Melnikov, B.Ye. Structure Effect on Viscoelastic Properties of Geosynthetic Material. *Magazine of Civil Engineering*. 2015. No. 4(56). Pp. 11–18. DOI: 10.5862/MCE.56.2 (rus)
10. Hui, Zhou, Yanshuang, Yang, Chuanqing, Zhang, Dawei, Hu. Experimental investigations on loading-rate dependency of compressive and tensile mechanical behaviour of hard rocks. *European Journal of Environmental and Civil Engineering*. 2015. Vol. 19. No. s1. Pp. s70–s82.
11. Laminelghil, Ameur, Guillaume, Robin, Mahdia, Hattab. Elastic properties in a clayey material under mechanical loading – an estimation through ultrasonic propagations. *European Journal of Environmental and Civil Engineering*. 2016. Vol. 20. No. 9. Pp. 1127–1146.
12. Chow, S.H., O'loughlin, C.D., Randolph, M.F. Soil strength estimation and pore pressure dissipation for free-fall piezocone in soft clay. *Géotechnique*. 2014. Vol. 64. No. 10. Pp. 817–827.
13. Kostas, Senetakis, Anastasios, Anastasiadis, Kyriazis, Ptilakis. Normalized shear modulus reduction and damping ratio curves of quartz sand and rhyolitic crushed rock. *Soils and Foundations*. 2013. Vol. 53. No. 6. Pp. 879–893.
14. Yumin, Chen, Hanlong, Liu, Haiqing, Wu. Laboratory study on flow characteristics of liquefied and post-liquefied sand. *European Journal of Environmental and Civil Engineering*. 2013. Vol. 17. No. s1. Pp. s23–s32.
15. Maheshwari, B., Kale, S., Kaynia, A. Dynamic properties of Solani sand at large strains: a parametric study. *International Journal of Geotechnical Engineering*. 2012. Vol. 6. No. 3. Pp. 353–358.
16. Cengiz, Kurtulus, Maral, Üçkardeş, Umut, Sarır, Onur Güner, Ş. Experimental studies in wave propagation across a jointed rock mass. *Bulletin of Engineering Geology and the Environment*. 2011. Vol. 71. No. 2. Pp. 231–234.
17. Wang, Y., Li, X., Zheng, B. Experimental study on mechanical properties of clay soil under compression by ultrasonic test. *European Journal of Environmental and Civil Engineering*. 2018. Vol. 22. No. 6. Pp. 666–685.
18. Verrucci, L., Lanzo, G., Tommasi, P., Rotonda, T. Cyclic and dynamic behaviour of a soft pyroclastic rock. *Géotechnique*. 2015. Vol. 65. No. 5. Pp. 359–373.
19. Vovk, A.A., Zamyshlyayev, B.V., Yevterev, L.S., Belinskiy, I.V., Mikhalyuk, A.V. Povedeniye gruntov pod deystviyem impulsivnykh nagruzok [Behavior of Soils under the Influence of Impulse Loads]. Kiyev: Naukova dumka, 1984. 286 p. (rus)
20. Zamyshlyayev, B.V., Yevterev, L.S. Modeli dinamicheskogo deformirovaniya i razrusheniya gruntovykh sred [Models of Dynamic Strain and Damage of Soil Medium]. Moscow: Nauka, 1990. 216 p. (rus)
21. Rykov, G.V., Skobeyev, A.M. Izmereniye napryazheniy v gruntakh pri kratkovremennykh nagruzkakh [Stress Measurement in Soils under Short-Term Loads]. Moscow: Nauka, 1978. 168 p. (rus)
22. Lyakhov, G.M. Osnovy dinamiki vzryvnykh voln v gruntakh i gornykh porodakh [Fundamentals of the Dynamics of Blast Waves in Soils and Rocks]. Moscow: Nedra, 1974. 192 p. (rus)
23. Sultanov, K.S. Volnovaya teoriya seysmostoykosti podzemnykh sooruzheniy [Wave Theory of Seismic Resistance of Underground Structures]. Tashkent: Fan, 2016. 392 p. (rus)
24. Mojtaba, E.Kan, Hossein, Taiebat, Nasser, Khalili. A Simplified Mapping Rule for Bounding Surface Simulation of 2 Complex Loading Paths in Granular Materials. *International Journal of Geomechanics*. 2014. Vol. 14. No. 2. Pp. 239–253.
25. Giuseppe, Buscarnera, Giuseppe, Dattola. Mathematical capture of failure processes in elastoplastic geomaterials. *Soils and Foundations*. 2016. Vol. 56. No. 1. Pp. 1–18.
26. Monnet, J. Elasto-plastic analysis of the pressuremeter test in granular soil. Part I: theory. *European Journal of Environmental and Civil Engineering*. 2012. Vol. 16. No. 6. Pp. 699–714.
27. Monnet, J. Elasto-plastic analysis of the pressuremeter test in granular soil. Part 2: numerical study. *European Journal of Environmental and Civil Engineering*. 2012. Vol. 16. No. 6. Pp. 715–729.
28. Shashkin, A.G. Modeling the performance of masses of weak clayey soils. *Soil Mechanics and Foundation Engineering*. 2011. Vol. 48. No. 4. Pp. 138–147.

29. Mirsayapov, I.T., Koroleva, I.V. Strength and deformability of clay soil under different triaxial load regimes that consider crack formation. *Soil Mechanics and Foundation Engineering*. 2016. Vol. 53. No. 1. Pp. 5–11.
30. Levandovskiy, A.N., Melnikov, B.E., Shamkin, A.A. Modeling of porous material fracture. *Magazine of civil Engineering*. 2017. No. 1 (69). Pp. 3–22.
31. Kalugina, Ju.A., Keck, D., Pronozin, Ya.A. Determination of soil deformation moduli after National Building Codes of Russia and Germany. *Magazine of civil Engineering*. 2017. No. 7 (75). Pp. 139–149.
32. Sultanov, K.S. A Non-Linear Law of the Deformation of Soft Soil. *Journal Applied Mathematics and Mechanics*. 1998. Vol. 62. No. 3. Pp. 465–472.
33. Sultanov, K.S., Khusanov, B.E. State equation for Soils Prone to Slump-type Settlement with Allowance for Degree of Wetting. *Soil Mechanics and Foundation Engineering*. 2001. Vol. 38. No. 3. Pp. 80–86.
34. Lyakhov, G.M. *Volny v gruntakh i poristykh mnogokomponentnykh sredakh [Waves in Soils and Porous Multi-Component Media]*. Moscow: Nauka, 1982. 238 p. (rus)
35. Sultanov, K.S., Khusanov, B.E. Determination of the Slump-Type Settlement of a Nonlinearly Deformable Soil Mass during Wetting. *Soil Mechanics and Foundation Engineering*. 2002. Vol. 39. No. 3. Pp. 81–84.
36. Sultanov, K.S. The Attenuation of Longitudinal Waves in Non-Linear Visco-Elastic Media. *Journal Applied Mathematics and Mechanics*. 2002. Vol. 66. No. 1. Pp. 115–122.
37. Mirsaidov, M.M., Godovannikov, A.M. *Seysmostoykost sooruzheniy [Seismic Stability of Structures]*. Tashkent: Uzbekistan, 2008. 220 p. (rus)
38. Mirsaidov, M.M. *Teoriya i metody rascheta gruntovykh sooruzheniy na prochnost i seysmostoykost [Theory and Methods of Calculation of Soil Structures for Strength and Seismic Resistance]*. Tashkent: Fan, 2010. 312 p. (rus)

Contacts:

Karim Sultanov, +998909702535; sultanov.karim@mail.ru
Pavel Loginov, +998909801765; lopavi88@mail.ru
Sabida Ismoilova, +998946204598; ismailova.sabida@mail.ru
Zulfiya Salikhova, +998909296665; zulfiya6665@gmail.com

© Sultanov, K.S., Loginov, P.V., Ismoilova, S.I., Salikhova, Z.R., 2019



DOI: 10.18720/MCE.85.7

Квазистатичность процесса динамического деформирования грунтов

К.С. Султанов*, **П.В. Логинов**, **С.И. Исмоилова**, **З.Р. Салихова**

*Институт механики и сейсмостойкости сооружений Академии наук Республики Узбекистан,
г. Ташкент, Узбекистан*

* E-mail: sultanov.karim@mail.ru

Ключевые слова: грунт, динамическое нагружение, волны, напряжения, квазистатика, механические характеристики грунтов.

Аннотация. Механические характеристики грунтов при их статическом и динамическом деформировании определяются экспериментально. Точность и достоверность определения механических характеристик грунтов при динамических нагружениях зависит от квазистатичности процесса деформирования грунта. Для этого необходимо обеспечить независимости результатов опытов от волновых процессов в грунте при воздействии на нее динамических нагрузок. Существуют лабораторные установки динамических нагружений (УДН) для проведения опытов по определению законов динамического деформирования, и на их основе механических характеристик грунтов. Проверка квазистатичности процесса динамического деформирования грунта в УДН, достигается решением соответствующей к постановке эксперимента волновой задачи. В связи с этим, рассмотрена задача о распространении плоской волны в грунте, постановка которой адекватно к постановке эксперимента на УДН. Для описания динамического деформирования грунтов принята упруго – вязкопластическая модель Г.М. Ляхова. Система дифференциальных уравнений в частных производных гиперболического типа, описывающая волновой процесс в грунте, решена методом характеристик с последующим применением численного метода конечных разностей по неявной схеме. Численным решением получены изменения параметров волн (напряжения, деформация и скорости частиц) по времени для разных сечений грунтового слоя. Показаны влияния толщины слоя грунта в УДН на параметры волн, следовательно, на квазистатичность процесса динамического деформирования грунтов в экспериментах. Определены также, степени количественного и качественного влияния механических характеристик грунта на параметры волн. На основе анализа полученных результатов установлена, что главными факторами определяющими квазистатичность волнового процесса являются – толщина грунтового слоя в УДН и параметры динамической нагрузки. Показана зависимость механических характеристик грунта от квазистатичности динамического деформирования грунтового слоя в УДН. Получена на основе результатов численного решения волновой задачи и их анализа условия обеспечения квазистатичности процесса деформирования образца грунта при ее динамическом сжатии в УДН.

Литература

1. Qingfend L., Chengrui C., Benhai Z., Bo M. Loess Soil Stabilization by Means of SiO₂ Nanoparticles // Soil Mechanics and Foundation Engineering. 2017. Vol. 54. No.6. Pp. 409–413.
2. Нгуен Ф.З. Исследования зависимости прочностных свойств грунта от его физического состояния // Инженерно-строительный журнал. 2012. № 9 (35). С. 23–28.
3. Гольдин А.Л., Нгуен Фьюнг Зунг. Построение траектории напряжений для ненасыщенного грунта при консолидированно-недренированных испытаниях в стабилометре // Инженерно-строительный журнал. 2012. № 9 (35). С. 35–40.
4. Morton J.P., O'Loughlin C.D., White D.J. Estimation of soil strength in fine-grained soils by instrumented free-fall sphere tests // Géotechnique. 2016. Vol. 66. No. 12. Pp. 959–968.
5. Chow S.H., Airey D.W. Soil strength characterisation using free-falling penetrometers // Géotechnique. 2013. Vol. 63. No. 13. Pp. 1131–1143.
6. Tadao E. Effects of grading and particle characteristics on small strain properties of granular materials // Soils and Foundations. 2016 Vol. 56. No. 4. Pp. 745–750.
7. Ignatova O.I. Deformation characteristics of the Jurassic clayey soils of Moscow // Soil Mechanics and Foundation Engineering. 2009. Vol. 46. No. 5. Pp. 196–201.

8. Александров А.С. Пластическое деформирование гранодиортового щебня и песчано-гравийной смеси при воздействии трехосной циклической нагрузки // Инженерно-строительный журнал. 2013. № 4 (39). С. 22–34.
9. Логинова И.И., Артомонова Д.А., Столяров О.Н., Мельников Б.Е. Влияние структуры на вязкоупругие свойства геосинтетических материалов // Инженерно-строительный журнал. 2015. № 4 (56). С. 11–18. DOI: 10.5862/MCE.56.2
10. Hui Zhou, Yanshuang Yang, Chuangqing Zhang, Dawei Hu. Experimental investigations on loading-rate dependency of compressive and tensile mechanical behaviour of hard rocks // European Journal of Environmental and Civil Engineering. 2015. Vol. 19. No. s1. Pp. s70–s82.
11. Laminelghil Ameer, Guillaume Robin, Mahdia Hattab. Elastic properties in a clayey material under mechanical loading – an estimation through ultrasonic propagations // European Journal of Environmental and Civil Engineering. 2016. Vol. 20. No. 9. Pp. 1127–1146.
12. Chow S.H., O'loughlin C.D., Randolph M.F. Soil strength estimation and pore pressure dissipation for free-fall piezocone in soft clay // Géotechnique. 2014. Vol. 64. No. 10. Pp. 817–827.
13. Kostas Senetakis, Anastasios Anastasiadis, Kyriazis Pitilakis. Normalized shear modulus reduction and damping ratio curves of quartz sand and rhyolitic crushed rock // Soils and Foundations. 2013. Vol. 53. No. 6. Pp. 879–893.
14. Yumin Chen, Hanlong Liu, Haiqing Wu. Laboratory study on flow characteristics of liquefied and post-liquefied sand // European Journal of Environmental and Civil Engineering. 2013. Vol. 17. No. s1. Pp. s23–s32.
15. Maheshwari B., Kale S., Kaynia A. Dynamic properties of Solani sand at large strains: a parametric study // International Journal of Geotechnical Engineering // 2012. Vol. 6. No. 3. Pp. 353–358.
16. Cengiz Kurtulus, Maral Üçkardeş, Umut Sarır, Ş. Onur Güner. Experimental studies in wave propagation across a jointed rock mass // Bulletin of Engineering Geology and the Environment. 2011. Vol. 71. No. 2. Pp. 231–234.
17. Wang Y., Li X., Zheng B. Experimental study on mechanical properties of clay soil under compression by ultrasonic test // European Journal of Environmental and Civil Engineering. 2018. Vol. 22. No. 6. Pp. 666–685.
18. Verrucci L., Lanzo G., Tommasi P., Rotonda T. Cyclic and dynamic behaviour of a soft pyroclastic rock // Géotechnique. 2015. Vol. 65. No. 5. Pp. 359–373.
19. Вовк А.А., Замышляев Б.В., Евтерев Л.С., Белинский И.В., Михалюк А.В. Поведение грунтов под действием импульсивных нагрузок. Киев: Наукова думка, 1984. 286 с.
20. Замышляев Б.В., Евтерев Л.С. Модели динамического деформирования и разрушения грунтовых сред. М.: Наука, 1990. 216 с.
21. Рыков Г.В., Скобеев А.М. Измерение напряжений в грунтах при кратковременных нагрузках. М.: Наука, 1978. 168 с.
22. Ляхов Г.М. Основы динамики взрывных волн в грунтах и горных породах. М.: Недра, 1974. 192 с.
23. Султанов К.С. Волновая теория сейсмостойкости подземных сооружений. Ташкент: Фан, 2016. 392 с.
24. Mojtaba E. Kan, Hossein Taiebat, Nasser Khalili. A Simplified Mapping Rule for Bounding Surface Simulation of 2 Complex Loading Paths in Granular Materials // International Journal of Geomechanics. 2014. Vol. 14. No. 2. Pp. 239–253.
25. Giuseppe Buscarnera, Giuseppe Dattola. Mathematical capture of failure processes in elastoplastic geomaterials // Soils and Foundations. 2016. Vol. 56. No. 1. Pp. 1–18.
26. Monnet J. Elasto-plastic analysis of the pressuremeter test in granular soil. Part I: theory // European Journal of Environmental and Civil Engineering. 2012. Vol. 16. No. 6. Pp. 699–714.
27. Monnet J. Elasto-plastic analysis of the pressuremeter test in granular soil. Part 2: numerical study // European Journal of Environmental and Civil Engineering. 2012. Vol. 16. No. 6. Pp. 715–729.
28. Shashkin A.G. Modeling the performance of masses of weak clayey soils // Soil Mechanics and Foundation Engineering. 2011. Vol. 48. No. 4. Pp. 138–147.
29. Mirsayapov I.T., Koroleva I.V. Strength and deformability of clay soil under different triaxial load regimes that consider crack formation // Soil Mechanics and Foundation Engineering. 2016. Vol. 53. No. 1. Pp. 5–11.
30. Levandovskiy A.N., Melnikov B.E., Shamkin A.A. Modeling of porous material fracture // Magazine of civil Engineering. 2017. No. 1 (69). Pp. 3–22.
31. Kalugina Ju., A., Keck D., Pronozin Ya., A. Determination of soil deformation moduli after National Building Codes of Russia and Germany // Magazine of civil Engineering. 2017. No. 7 (75). Pp. 139–149.
32. Sultanov K.S. A Non-Linear Law of the Deformation of Soft Soil // Journal Applied Mathematics and Mechanics. 1998. Vol. 62. No. 3. Pp. 465–472.
33. Sultanov K.S., Khusanov B.E. State equation for Soils Prone to Slump-type Settlement with Allowance for Degree of Wetting // Soil Mechanics and Foundation Engineering. 2001. Vol. 38. No.3. Pp. 80–86.
34. Ляхов Г.М. Волны в грунтах и пористых многокомпонентных средах. М.: Наука, 1982. 238 с.
35. Sultanov K.S., Khusanov B.E. Determination of the Slump-Type Settlement of a Nonlinearly Deformable Soil Mass during Wetting // Soil Mechanics and Foundation Engineering. 2002. Vol. 39. No. 3. Pp. 81–84.
36. Sultanov K.S. The Attenuation of Longitudinal Waves in Non-Linear Visco-Elastic Media // Journal Applied Mathematics and Mechanics. 2002. Vol. 66. No.1. Pp.115–122.
37. Мирсаидов М.М., Годованников А.М. Сейсмостойкость сооружений. Ташкент: Узбекистан, 2008. 220 с.
38. Мирсаидов М.М. Теория и методы расчета грунтовых сооружений на прочность и сейсмостойкость. Ташкент: Фан, 2010. 312 с.

Контактные данные:

Карим Султанович Султанов, +998909702535; эл. почта: sultanov.karim@mail.ru

Павел Викторович Логинов, +998909801765; эл. почта: lopavi88@mail.ru

Сабида Исроиловна Исмоилова, +998946204598; эл. почта: ismailova.sabida@mail.ru

Зулфия Рустамовна Салихова, +998909296665; эл. почта: zulfiya6665@gmail.com

© Султанов К.С., Логинов П.В., Исмоилова С.И., Салихова З.П., 2019